High-spectral-resolution attosecond absorption spectroscopy of autoionization in xenon

Birgitta Bernhardt,[1,2,*] Annelise R. Beck,[1,2] Xuan Li,[1] Erika R. Warrick,[1,2] M. Justine Bell,[1,2] Daniel J. Haxton,[1] C. William McCurdy,[1,3] Daniel M. Neumark,[1,2] and Stephen R. Leone[1,2,4]

[1]*Ultrafast X-ray Science Laboratory, Chemical Sciences Division, Lawrence Berkeley National Laboratory, Berkeley, California 94720, USA*

[2]*Department of Chemistry, University of California, Berkeley, California 94720, USA*

[3]*Department of Chemistry, University of California, Davis, California 95616, USA*

[4]*Department of Physics, University of California, Berkeley, California, USA*

(Received 25 November 2013; published 10 February 2014)

The decay of highly excited states of xenon after absorption of extreme ultraviolet light is directly tracked via attosecond transient absorption spectroscopy using a time-delayed near-infrared perturbing pulse. The lifetimes of the autoionizing $5s5p^6 6p$ and $5s5p^6 7p$ channels are determined to be (21.9 ± 1.3) fs and (48.4 ± 5.0) fs, respectively. The observed values support lifetime estimates obtained by traditional linewidth measurements. The experiment additionally obtains the temporal evolution of the decay as a function of energy detuning from the resonance center, and a quantum mechanical formalism is introduced that correctly accounts for the observed energy dependence.

DOI: 10.1103/PhysRevA.89.023408 PACS number(s): 32.80.Zb, 32.80.Aa, 42.50.Md

Highly excited many-electron atomic or molecular systems relax to states of lower energy by electronic rearrangement. The rotational and vibrational dynamics associated with these transitions have been successfully tracked with femtosecond lasers [1]. These experiments often make use of transient absorption spectroscopy, where the sample absorbance over a range of frequencies is detected as a function of time after excitation by a laser pulse [2]. However, only attosecond pulses [3] enable time domain access to electron dynamics, the fundamental driver of atomic and molecular processes including chemical reactions, ionization phenomena, and nonadiabatic dynamics. The recent development of attosecond transient absorption (ATA) allows one to apply the power and generality of transient absorption to these much faster dynamics, enabling, for example, the observation of electron wave-packet dynamics in gases [4] and the time evolution of electronic excitations in solids [5].

In this article, we present how to systematically apply ATA to measure the time dynamics of processes such as autoionization in gases. Autoionization was observed in the photoabsorption spectra of rare gas atoms for the first time in the 1930s [6] and its characteristic asymmetric line shapes were attributed to a quantum interference coupling of autoionizing bound states with the continuum of states by Fano [7]. Since then, Fano profiles, linewidths, and lineshapes have been widely studied at synchrotron radiation facilities [8,9], and more recently with tabletop high-harmonic generation setups [10]. The excited-state lifetimes are deduced from the measured resonance widths of the static absorption features. However, various possible broadening mechanisms such as Doppler, pressure [9], and power broadening [11], as well as congestion of multiple resonance features complicate lifetime determinations, which thus depend on the precise knowledge of several parameters and only yield a lower bound.

The first experiment that took advantage of attosecond laser pulses to measure lifetimes quantified the Auger decay of an M-shell vacancy in krypton [12]. The lifetime of (7.9 ± 1) fs was deduced by a "streaking" analysis [13] for the emission of photoelectrons in the presence of a dressing laser field. This experiment has not been established as a common method for direct lifetime measurements, possibly because of the complexity of the photoelectron spectra in such pump-probe experiments, the influence of the streaking field, and the limited spectral resolution of photoelectron spectrometers [14].

Recently, the first demonstration of tracking autoionization in argon with transient absorption spectroscopy investigated the modification in shape, linewidth, strength, and position of the resonances induced by a strong infrared laser pulse. It also yielded consistent fits of the transient absorbance at the resonances if the approximate lifetime obtained from the linewidth was used as a fixed input parameter [15]. In that pioneering experiment, as well as in the present setup, an attosecond extreme ultraviolet (XUV) field induces a time-dependent polarization in the gas sample, i.e., it stimulates a transient oscillating dipole moment [16] connecting the ground and excited states within the spectral bandwidth of the pulse. A near-infrared (NIR) field modifies the induced polarization, resulting in depletion of the autoionizing states by coupling to neighboring bound states or to continuum states. A spectrometer detects the integral of the interference of the transmitted XUV field and the field radiated by the induced dipole at various time delays between XUV and NIR pulse.

Here, we present direct lifetime measurements by applying ATA to the $5s5p^6 6p$ and $5s5p^6 7p$ autoionizing states in xenon. We confirm the values derived from traditional linewidth measurements [8], and establish how ATA can be reliably used as a general method to measure highly excited-state lifetimes. The absorbance signal on resonance center decays with twice the lifetime, as expected from the basic relationship between polarization and population [17]. Moreover, the method presented here combines subfemtosecond temporal resolution with ≈10 meV spectral resolution, allowing for a detailed photon-energy-dependent investigation of the absorption dynamics. While previous transient absorp-

*BCBernhardt@lbl.gov

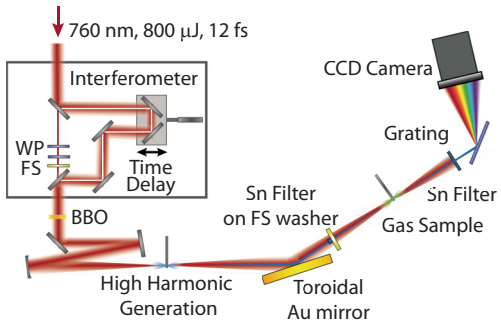

FIG. 1. (Color online) Experimental setup for transient absorption spectroscopy in xenon. WP: wave plate, FS: fused silica plate, BBO: crystal for second-harmonic generation.

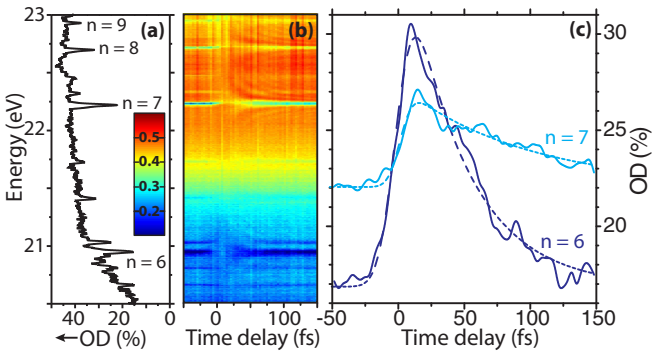

FIG. 2. (Color online) (a) Static XUV absorbance spectrum of the $5s5p^6np$ autoionizing states in xenon. (b) XUV absorbance spectrum of xenon in a strong NIR laser field with an intensity of 1.3×10^{12} W/cm^2. Negative time delays correspond to the NIR pulse arriving before the XUV pulse at the target. (c) Line-out (solid line) and fit (dashed line) of the $n = 6$ (dark blue) and $n = 7$ (light blue) resonances; see text for details.

tion experiments and analysis have focused on the dynamics occurring exactly on an atomic resonance [15,18], we use experiment and theory to characterize the modified temporal evolution of the absorbance along the asymmetric Fano-shaped wings of the spectral features.

Figure 1 shows the vacuum apparatus and associated XUV optics used in this experiment, both of which have been modified from a previous setup [19,20]. A commercial Ti:sapphire chirped pulse amplifier system produces 25-fs NIR pulses centered at 760 nm with a repetition rate of 1 kHz. This output is spectrally broadened via self-phase modulation in a hollow-core fiber filled with neon and the pulses are subsequently compressed to 12 fs by chirped mirrors. An interferometer configuration with two annular splitting and combining mirrors separates the beam into an inner arm for the conversion into attosecond XUV pulses and a doughnut-shaped outer arm for the perturbing few-cycle NIR pulses. The inner beam is sent through a half- and quarter-wave plate and a BBO crystal for second-harmonic generation. This combination is used for double optical gating [21], a technique that enables isolated attosecond pulse generation for relatively long initial laser pulses. A delay stage in the outer arm of the interferometer introduces the adjustable delay between the XUV and NIR pulses for the ATA scheme.

After the two beams are recombined, they are focused into the high-harmonic target chamber. Only the inner arm is intense enough to generate XUV radiation for the production of attosecond pulses via high-harmonic generation [22], using here a krypton-filled gas cell with small-aperture open ends. Since the XUV and NIR beams are copropagating, the residual infrared light of the inner beam is rejected by the 200-nm-thick Sn filter attached to a 1-mm-thick doughnut-shaped fused silica (FS) plate. After passing through the Sn filter, the XUV spectrum spans about 19–23 eV. The corresponding pulse duration was previously characterized with a 750-nm streak field to be about 400 as in [19]. Dispersion and delay introduced by the FS washer are balanced by a FS plate placed in the inner arm of the interferometer.

A gold-coated toroidal mirror (radii of curvature: $R_1 = 5758$ mm and $R_2 = 174$ mm, angle of incidence: 10°) focuses in grazing incidence the XUV and NIR beams into the sample cell containing xenon gas (interaction length: nominally 1 mm). The backing pressure was maintained low enough so that propagation effects in the sample are negligible [17]). After the target cell, another 300-nm-thick Sn filter suppresses the NIR radiation. The remaining XUV absorption spectrum is dispersed with a grating (Hitachi, 01-0464) and detected with a charge-coupled device (CCD) camera (Pixis-XO 400B). The spectrometer resolution was determined to be 13 meV by a helium reference absorption line measurement. The $1s2p$ (21.218 eV), $1s3p$ (23.087 eV), and $1s4p$ (23.743 eV) resonance peaks in helium were used to calibrate the spectrometer [23].

Figure 2(a) shows the static optical density $\mathrm{OD} = -\log_{10}(I_t/I_0)$ of xenon in the absence of the NIR pulse, where I_0 is the measured XUV intensity without xenon and I_t is the XUV intensity transmitted through the gas sample. The $5s5p^6np$ autoionizing states with n={6,7,8,9} are clearly visible as window resonances [24] superimposed on a continuous absorption background. Figure 2(b) depicts the optical density for different time delays between the XUV and the NIR pulse, averaged over 20 time scans with 2 s of integration time for each delay step. A step size of 3 fs was chosen for convenience; smaller values down to 60 as are nevertheless possible. Negative values in the time delay correspond to NIR pulses arriving before the XUV pulses at the gas sample. Figures 2(a) and 2(b) also show weaker resonance peaks between the autoionizing states that have been attributed to two electron transitions [8,25]. Near zero time delay, where the XUV and NIR pulses overlap, all window resonance peaks are broadened and weakened, resulting in a higher optical density. Figure 2(c) shows the absorbance line-outs closest to the expected $5s5p^66p$ (20.956 eV) and $5s5p^67p$ (22.220 eV) resonance centers as a function of time delay (the respective NIST database entries are 20.951 and 22.226 eV [23]).

Figure 2(c) also shows the corresponding fit functions on line center, a convolution of a Gaussian function for the perturbing NIR pulse with an exponential decay for the polarization decay. The experimental decay times of the polarization signal are found to be (43.8 ± 2.6) fs for the $6p$ state and (96.8 ± 10.0) fs for the $7p$ state, respectively. These polarization decays should follow the decay of the excited-state wave function, not the population, and are therefore twice as

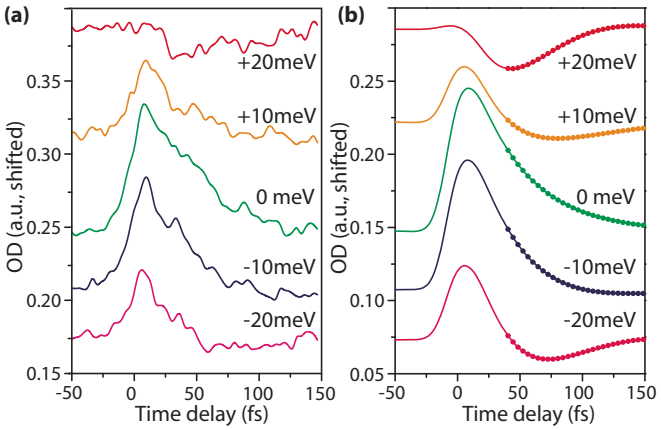

FIG. 3. (Color online) (a) Xenon absorbance dependent on different time delays between XUV and NIR and at different energies around the xenon $5s5p^6 6p$ autoionizing resonance. 0 meV is considered the line center. (b) Corresponding simulated absorbance curves calculated with a three-state model (solid line) and with Eq. (3) (dots; see text for details).

long as the lifetimes for population decay (see below). Hence, the excited-state lifetimes are (21.9 ± 1.3) fs for the $6p$ and (48.4 ± 5.0) fs for the $7p$ state. Similar to [15], we observe an enhancement of the perturbation effects caused by the NIR pulse with increasing NIR intensities (10^{11}–10^{13} W/cm^2). However, the exponential decay rates of the respective states are unmodified, proving that the perturbing NIR pulse does not influence the state population decay itself.

Figure 3(a) shows the absorption line-outs in spectral windows that are either blue- or redshifted from the $6p$ resonance center. Compared to resonant excitation, the polarization appears to decay more rapidly, and with increasing energy detuning, dramatic changes of the temporal evolution are observed.

There are two notable aspects to the results. First, the time constants for the decay of the on-resonance ATA signals in Fig. 2(c) are obtained independently without any assumption of values from previous linewidth measurements. In Ref. [8], the Fano linewidths Γ were found to be (31.2 ± 0.8) meV for the $6p$ and (13.0 ± 0.6) meV for the $7p$ state, respectively. By using the relation $\tau = \frac{\hbar}{\Gamma}$, the corresponding state lifetimes τ are obtained as (21.1 ± 0.5) fs and (50.6 ± 2.3) fs. These are in good agreement with the measurement here, justifying the validity of lifetimes determined by ATA. Secondly, the subfemtosecond temporal resolution is augmented by meV spectral resolution, providing two-dimensional insight into the polarization dynamics that are measured by ATA. The marked dependence of the off-resonant ATA signals on energy detuning in Fig. 3(a) has not been discussed previously to this extent but has been pointed out in Ref. [26].

In order to interpret the experimentally measured data shown in Fig. 3(a), a three-state model calculation is performed that aims to describe the basic physical process of the NIR detection of time behaviors: An ultrashort XUV pulse is applied at $t = 0$ and a subsequent NIR pulse [full width at half maximum (FWHM) = 24 fs] is applied at time delay $t = t_d$, which couples the resonance state to an ionization continuum, the implementation of which is similar to Ref. [27]. We evaluate the induced dipole by $d(t) = \langle \Psi(t)|\hat{d}|\Psi(t)\rangle$, where Ψ(t) is the time-dependent wave packet and is calculated by solving the time-dependent Schrödinger equation describing such a three-state system coupled by the XUV and NIR pulses. The photon absorption spectrum [28] is calculated via $S(\omega) = 2\mathrm{Im}[d(\omega)\varepsilon^*(\omega)]$, where $d(\omega)$ and $\varepsilon(\omega)$ are the Fourier transforms of the time-dependent dipole, $d(t)$, and the electric field, $\varepsilon(t)$, respectively. For different XUV photon energies, ω, we define a detuning variable $\Delta\omega = E_2 - E_1 - \omega$. The model simulation results are plotted in Fig. 3(b) for the values $\Delta\omega = -20$, -10, 0, $+10$, and $+20$ meV, respectively. The spectral resolution of 13 meV has not been considered here because of its negligible impact on the experimental lifetime measurements of the relatively broad resonance states. The theoretical model agrees qualitatively with the absorption changes versus detunings observed in the experiment [Fig. 3(a)]. References [27,29] consider the autoionizing state coupled to both a continuum and a discrete state (also coupled to each other via field-free relaxation processes). However, the current study explicitly distinguishes these two coupling mechanisms and considers them separately, which is equivalent to a systematic study of varying the Fano parameter corresponding to the NIR field coupling from 0 to infinity.

These results are further supported by a more analytical mathematical discussion of the absorbance dynamics. The wave function of the system after XUV excitation is

$$\Psi(t) = c_1(t)e^{-iE_1 t}|1\rangle + c_2(t)e^{-iE_2 t-\Gamma t/2}|2\rangle, \qquad (1)$$

where $|1\rangle$ and $|2\rangle$ are the wave functions of the ground state E_1 and the excited state E_2, respectively, while Γ is the width of the resonance state whose inverse is its lifetime. Initially, the system is in its ground state and thus $c_1(t < 0) = 1$ and $c_2(t < 0) = 0$. Assuming a "sudden approximation," where both the first XUV pulse and the subsequent, assumed complete, annihilation process induced by the NIR pulse are short, the time-dependent dipole $d(t)$ induced by the XUV pulse can be expressed as

$$\begin{aligned} d(t) &= \langle \Psi(t)|\hat{d}|\Psi(t)\rangle \\ &= d_{12}c_1^*(t)c_2(t)e^{-i(E_2-E_1-\frac{i\Gamma}{2})t} + \text{c.c.}, \\ &\propto \begin{cases} 0, & t < 0 \\ i\varepsilon_0 d_{12}^2 e^{-i(E_2-E_1-\frac{i\Gamma}{2})t} + \text{c.c.}, & 0 < t < t_d \\ 0, & t_d < t \end{cases} \end{aligned} \qquad (2)$$

Here, the coefficients c_1 and c_2 are found by applying the time-dependent Schrödinger equation to Eq. (1); ε_0 is the electric field strength of the ultrashort XUV pulse, d_{12} is the transition dipole coupling between the two states by the XUV, and t_d is the time delay between the XUV and NIR pulse.

The photon absorption spectrum is obtained via $S(\omega) = 2\mathrm{Im}[d(\omega)\varepsilon^*(\omega)]$. Note that the Fourier transform of $d(t)$ from Eq. (2) leads to an overall dependence of $\exp[-\Gamma^* t_d/2]$ times an oscillatory factor depending on detuning, $\exp[-i\Delta\omega^* t_d]$. The final expression for $S(\omega)$ that follows from Eq. (2) is then given by

$$S(\omega) = 2\mathrm{Im}[d(\omega)\varepsilon^*(\omega)] = A - Be^{-\Gamma t_d/2}\cos[\Delta\omega t_d + \varphi], \qquad (3)$$

where A, B, φ depend on the laser parameters and the atomic properties, but not on the delay time t_d. Equation (3) is the key analytical result, reproducing the factor of 2 for the lifetime determination and describing the off-resonant behavior of the absorbance. In particular, in Fig. 3(b) for $t_d \geqslant 40$ fs, when the overlap between the XUV and NIR fields is small, the three-state model results (solid lines) for $S(t_d; \Delta\omega)$ fit the expression (filled circles) in Eq. (3), exactly. The expression for the photon absorption spectrum in Eq. (3) appears to be applicable to general cases that are under current investigation [30]. A similar finding with a different derivation for the induced polarization has been published recently [17]. The numerical three-state calculation used to produce the spectra in Fig. 3(b) differs from the model in Eq. (3), which is based on a sudden approximation, by employing a ramped NIR pulse and explicit coupling of the autoionizing state to the continuum.

An intuitive physical picture of the origin of the $\cos[\Delta\omega t_d + \varphi]$ behavior of the absorption spectrum can also be obtained in the limit of a sudden annihilation by the NIR pulse of the oscillating and decaying dipole originally induced by the XUV pulse. In that limit, the behavior is simply the ringing as a function of ω caused in $d(\omega)$ (the Gibbs phenomenon [31]) because it is the Fourier transform of a function that is sharply cut off at $t = t_d$.

In general, highly excited states with much shorter lifetimes than the xenon $6p$ and $7p$ states could be measured with the setup and method described; the rise time of the instrumental response function determines what polarization decay rates can be resolved. However, accurate extraction of the lifetime also depends on the noise in the time scan itself and the perturbation strength of the NIR pulse. Thus, the NIR intensity and the transition dipole strength of the investigated state play a role. With the present conditions, the instrumental rise time of 10 fs (corresponding to a NIR pulse duration of FWHM = 24 fs) allows the measurement of lifetimes down to 5 fs. This can be further improved by advanced tailoring of the chirped mirrors to compress the NIR pulses to a duration close to their Fourier limit (FWHM~6 fs).

Applying the time-resolved measurement of state lifetimes to molecules will further enlighten the coupling mechanisms of electronic and nuclear kinetics. For example, competing decay pathways from molecular excited states above the ionization potential such as autoionization and predissociation [25] could be studied with temporal resolution [32] and could give unprecedented insights into the reaction sequences that static measurements cannot disclose.

In conclusion, a general time-resolved lifetime measurement is presented for highly excited states, applied to autoionizing states in a gas by attosecond transient absorption. The measured values taken with our tabletop setup confirm the lifetime values that can be deduced from traditional energy-domain measurements and thus prove the viability of ATA. However, the time-resolved approach is unaffected by overlapping features that complicate energy-domain measurements. Additionally, we presented a rigorous treatment that accounts for the modified temporal evolution of the decay as a function of energy detuning from the resonance.

ACKNOWLEDGMENTS

This work was supported by the Director, Office of Science, Office of Basic Energy Sciences, and by the Division of Chemical Sciences, Geosciences, and Biosciences of the US Department of Energy at LBNL under Contract No. DE-AC02-05CH11231. B.B. gratefully acknowledges support by the Alexander von Humboldt foundation. A.R.B. acknowledges funding from NSF-GRFP. S.R.L. acknowledges support of the Office of the Secretary of Defense through the NSSEFF program. The authors thank Camilla Bacellar, Mike Ziemkiewicz, and He Wang for providing replacement optics on short notice.

[1] A. H. Zeweil, J. Phys. Chem. A **104**, 5660 (2000).
[2] Z.-H. Loh, C. H. Greene, and S. R. Leone, Chem. Phys. **350**, 7 (2008).
[3] F. Krausz and Corkum, Nat. Phys. **3**, 381 (2007).
[4] E. Goulielmakis, Z.-H. Loh, A. Wirth, R. Santra, N. Rohringer, V. S. Yakovlev, S. Zherebtsov, T. Pfeifer, A. M. Azzeer, M. F. Kling, S. R. Leone, and F. Krausz, Nature **466**, 5 (2010).
[5] M. Schultze, E. M. Bothschafter, A. Sommer, S. Holzner, W. Schweinberger, M. Fiess, M. Hofstetter, R. Kienberger, V. Apalkov, V. S. Yakovlev, M. I. Stockman, and F. Krausz, Nature **493**, 75 (2013).
[6] H. Beutler, Z. Phys. **93**, 177 (1935).
[7] U. Fano, Phys. Rev. **124**, 1866 (1961).
[8] D. L. Ederer, Phys. Rev. A **4**, 2263 (1971).
[9] R. Madden and K. Codling, J. Res. Natl. Bur. Stand., Sect. A **76**, 1 (1972).
[10] C. Ott, A. Kaldun, Raith, K. Meyer, M. Laux, J. Evers, C. H. Keitel, C. H. Greene, and T. Pfeifer, Science **340**, 716 (2013).
[11] N. Vitanov, B. Shore, L. Yatsenko, K. Böhmer, T. Halfmann, T. Rickes, and K. Bergmann, Opt. Commun. **199**, 117 (2001).
[12] M. Drescher, M. Hentschel, R. Kienberger, M. Uiberacker, V. Yakovlev, A. Scrinzi, T. Westerwalbesloh, U. Kleineberg, U. Heinzmann, and F. Krausz, Nature **419**, 803 (2002).
[13] M. Kitzler, N. Milosevic, A. Scrinzi, F. Krausz, and T. Brabec, Phys. Rev. Lett. **88**, 173904 (2002).
[14] C. D. Lin and W.-C. Chu, Phys. Rev. A **82**, 053415 (2010).
[15] H. Wang, M. Chini, S. Chen, C.-H. Zhang, F. He, Y. Cheng, Y. Wu, U. Thumm, and Z. Chang, Phys. Rev. Lett. **105**, 143002 (2010).
[16] W. T. Pollard and R. Mathies, Annu. Rev. Phys. Chem. **43**, 497 (1992).
[17] A. N. Pfeiffer, M. J. Bell, A. R. Beck, H. Mashiko, D. M. Neumark, and S. R. Leone, Phys. Rev. A **88**, 051402 (2013).
[18] Z. X. Zhao and C. D. Lin, Phys. Rev. A **71**, 060702 (2005).
[19] H. Mashiko, M. J. Bell, A. R. Beck, M. J. Abel, M. Nagel, C. P. Steiner, J. Robinson, D. M. Neumark, and S. R. Leone, Opt. Express **18**, 25887 (2010).
[20] M. J. Bell, A. R. Beck, H. Mashiko, D. M. Neumark, and S. R. Leone, J. Mod. Opt. **60**, 1506 (2013).
[21] H. Mashiko, S. Gilbertson, C. Li, S. D. Khan, M. M. Shakya, E. Moon, and Z. Chang, Phys. Rev. Lett. **100**, 103906 (2008).

[22] A. McPherson, G. Gibson, H. Jara, U. Johann, T. S. Luk, I. A. McIntyre, K. Boyer, and C. K. Rhodes, J. Opt. Soc. Am. B **4**, 595 (1987).
[23] A. Kramida, Y. Ralchenko, J. Reader *et al.*, NIST Atomic Spectra Database (ver. 5.1), (National Institute of Standards and Technology, Gaithersburg, MD, 2013). Available at http://physics.nist.gov/asd.
[24] T. Chang and T. Fang, Radiat. Phys. Chem. **70**, 173 (2004).
[25] D. Cubric, D. B. Thompson, D. R. Cooper, G. C. King, and F. H. Read, J. Phys. B **30**, L857 (1997).
[26] C. Ott, A. Kaldun, P. Raith, K. Meyer, M. Laux, Y. Zhang, S. Hagstotz, T. Ding, R. Heck, and T. Pfeifer, arXiv:1205.0519 [physics.atom-ph] (2012).
[27] W.-C. Chu and C. D. Lin, Phys. Rev. A **87**, 013415 (2013).
[28] M. Gaarde, C. Buth, J. L. Tate, and K. J. Schafer, Phys. Rev. A **83**, 013419 (2011).
[29] P. Lambropoulos and P. Zoller, Phys. Rev. A **24**, 379 (1981).
[30] X. Li, B. Bernhardt, A. R. Beck, E. R. Warrick, A. N. Pfeiffer, M. J. Bell, D. J. Haxton, C. W. McCurdy, D. M. Neumark, and S. R. Leone (unpublished).
[31] E. Hewitt and R. E. Hewitt, Arch. Hist. Exact Sci. **21**, 129 (1979).
[32] D. Strasser, L. H. Haber, B. L. Doughty, and S. R. Leone, Mol. Phys. **106**, 275 (2008).